

12

EUROPEAN PATENT APPLICATION

21 Application number: 89305663.0

51 Int. Cl.⁴ G01N 24/04

22 Date of filing: 05.06.89

30 Priority: 06.06.88 US 202624

43 Date of publication of application:
13.12.89 Bulletin 89/50

84 Designated Contracting States:
DE FR GB NL

71 Applicant: GENERAL ELECTRIC COMPANY
1, River Road
Schenectady NY 12345(US)

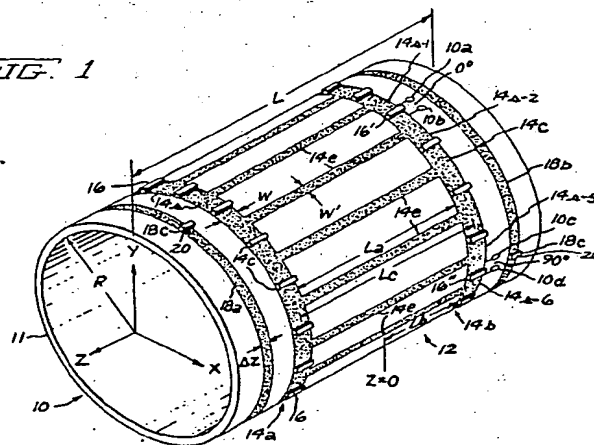
72 Inventor: Roemer, Peter Bernard
955 Saint David's Lane
Schenectady New York 12309(US)
Inventor: Bottomley, Paul Arthur
64 Pico Road
Clifton Park New York 12065(US)
Inventor: Edelstein, William Alan
850 Oregon Avenue
Schenectady New York 12309(US)

74 Representative: Pratt, Richard Wilson et al
London Patent Operation G.E. TECHNICAL
SERVICES CO. INC. Burdett House 15/16
Buckingham Street
London WC2N 6DU(GB)

54 RF coil for NMR.

57 A RF volume coil with optimized signal-to-noise ratio, for NMR use, has a reduced length L_c , which is between about $0.3r_s$ and about $1.5r_s$, where r_s is the radius of a sample-to-be-investigated, contained within the cylindrical volume coil, with the volume coil radius r_c being between about $1.0r_s$ and about $1.6r_s$. The "short" volume coil has an improved SNR for a voxel located substantially on the central plane of the coil, relative to the SNR of a "normal"-length volume coil with $L_c \geq 4r_s$.

FIG. 1



RF COIL FOR NMR

The present invention relates to a radio frequency (RF) coil, for example, for nuclear magnetic resonance (NMR) apparatus. A preferred embodiment of the invention provides a radio-frequency (RF) coil of the "birdcage" form, having optimized signal-to-noise ratio (SNR) particularly when receiving RF signals in a NMR imaging or spectroscopy environment.

It is now well known to image and obtain chemical shift spectra from certain nuclei, such as ^1H , ^{31}P and the like, to determine the internal distribution and chemical form of those nuclei in a specimen, using NMR. In particular, NMR imaging of a particular nuclear species in the human body has proven to be medically and scientifically significant. It is now also well known that substantial increases in SNR can be observed by increasing the static magnetic field B_0 in which the specimen-to-be-imaged is immersed. It has been found that attempts to reduce the size of a volume picture element (voxel) by trading off this SNR advantage, result in relatively little reduction of the linear voxel extent, since the voxel linear dimension is apparently proportional to the cube root of the signal-to-noise ratio. However, a SNR increase can be utilized to shorten the data acquisition time, with acquisition time reductions proportional to the square of the SNR increase being realizable. Accordingly, it is highly desirable to increase, to the greatest extent possible, the signal-to-noise ratio in a RF volume coil, and particularly in the form of RF volume coil known as a "birdcage" coil, which is one having a pair of conductive loop elements spaced along a common longitudinal axis, with each of the loop elements having a plurality of series-connected capacitance elements spaced along the loop peripheries, and with a like plurality of axial conductive elements electrically interconnecting the conductive loop elements at points between adjacent ones of the serially-connected capacitive elements, such as are described in U.S. Patents 4,680,548 and 4,692,705, respectively issued July 14, 1987 and September 8, 1987, and both incorporated herein in their entireties by reference.

In accordance with one embodiment of the invention, a RF volume coil with optimized signal-to-noise ratio, for NMR and the like use, has a reduced length L_c , which is between about $0.3r_s$ and about $1.5r_s$, where r_s is the effective radius of a sample-to-be-investigated, contained within the cylindrical volume coil, with the volume coil radius r_c being between about $1.0r_s$ and about $1.6r_s$. Such a "short" volume coil has an improved SNR for a voxel located substantially along the axis of the

coil, although the sensitivity S of the coil is non-uniform, especially for voxels removed from the coil axis, relative to the SNR of a "normal"-length volume coil with $L_c \geq 4r_s$.

In one presently preferred embodiment, an optimized SNR volume coil, of "birdcage" form, designed for detection of NMR response signals from ^{31}P nuclei at about 26MHz., has a length L_c of about $1.0r_s$ and a coil radius r_c of about $1.1r_s$, and has better than a 60 percent increase in SNR relative to a cylindrical volume coil, of the same form, having a length of about four times the sample radius. Operation of the detection coil in a true-quadrature mode, to detect only the circularly-polarized NMR field, contributes an additional SNR improvement of about 40 percent.

A better understanding of the present invention will become apparent upon reading of the following illustrative description, when considered in conjunction with the drawings, in which:-

Figure 1 is a perspective view of one presently preferred high-pass birdcage embodiment of the optimized volume RF coil of the present invention;

Figure 2 is a graph illustrating the relative signal-to-noise ratio of volume RF coils having fixed ratios of sample radius and coil radius, for varying coil lengths, and useful in appreciating the improvement of the present invention;

Figure 3 is a graph illustrating the relative sensitivity of the coil for voxels at various radial distances from the coil axis, for various axial positions within the coil, and also useful in appreciating the features of the present invention; and

Figure 4 is a perspective view of one presently preferred low-pass birdcage embodiment of the optimized volume RF coil of the present invention.

Referring initially to Figure 1, a volume RF coil assembly 10, is of cylindrical form, and is supported by a non-magnetic, non-conducting and non-dielectric tube 11, of acrylic and the like material, having a radius R and a length L , which for a coil for imaging of a human head are illustratively of about 5 inches and about 8 inches, respectively. The axis of the cylindrical coil form 11 is aligned with the Z axis of a Cartesian coordinate system, and with the center $Z=0$ of that system lying at the axial center of the coil 10. An antenna portion 12 of assembly 10 is comprised of first and second spaced-apart conductive loop elements 14a and 14b, each having a width W , here, about one-half inch, with the facing edges of conductors 14a and 14b having a spacing L_a here, about 4.5 inches,

such that the edge planes of conductors 14a and 14b are each at a distance L_c , here, about 2.25 inches, from the axial center $Z=0$ plane; the effective length L_c of the coil is about 5 inches. Each of conductors 14a and 14b is broken at each of a plurality N of locations, typically in axial alignment, by a small gap 14c so as to form a like plurality N of substantially identical conductive segments 14s. Advantageously, the number N of segments is represented by a power p of base 2, i.e. $N=2^p$, where $p=1, 2, 3, \dots$. In the illustrated embodiment, $p=4$ and $N=16$. Each of the 16 conductor gaps 14c is bridged with a serially-connected capacitive element 16. Each of a like plurality N of axial conductive elements 14e interconnect similarly disposed segments 14s of the first and second spaced-apart loop elements 14a and 14b; each axial conductive element 14e has a width W , here, about one-half inch. First and second conductive end rings 18a and 18b, if used, are formed in planes substantially parallel to the planes of loop elements 14, but axially extended therebeyond; each end ring is of thickness ΔZ (here, about one-half inch) and has at least one gap 18c therein, with each gap being bridged by an associated serially-connected capacitive element 20; the end rings tend to eliminate undesirable coil resonances.

This particular high-pass "birdcage" form of optimized-SNR volume RF coil 10 has a balanced feedpoint between first and second terminals 10a and 10b, which are connected across one of the capacitors 16, illustratively connected to adjacent conductive segments 14s-1 and 14s-2, respectively, and across capacitor 16'. Advantageously, the coil will be connected for quadrature excitation and/or reception, with a second balanced feedpoint being provided between third and fourth terminals 10c and 10d, which are connected to adjacent conductive segments 14s-5 and 14s-6, respectively, and across another capacitor 16'', which is situated in that part of coil loop 14b having a radial reference substantially at 90° to a radial reference extended from the cylinder axis to the first balanced input about capacitor 16'. The use of baluns, balanced multiple-half-wavelength cables, hybrid quadrature elements and the like, to couple the quadrature feedpoints to a single unbalanced reception cable, and the like configurations external to coil 10, are all well known to the art.

The operation of volume detection coil 10 can be analyzed by the principle of reciprocity, so that the RE coil 10 NMR signal-to-noise ratio ψ detected from a voxel located at a point (r, θ, z) in the cylindrical polar coordinate system, with origin $z=0$ at the coil center and with, as here, the Z axis coincident with the coil cylindrical axis, is

$$\psi \propto B_1(r, \theta, z) / \sqrt{R} \quad (1)$$

where B_1 is the transverse RF magnetic field pro-

duced by a unit current and R is the total noise resistance at the NMR angular frequency ω . In optimizing ratio ψ along the coil axis, the transverse RF magnetic field B_1 of a birdcage coil geometry with length L_c and radius r_c is, for a maximum end-ring 18 unity current, produced by sinusoidal current distributions J , so that

$$J = (-z \sin \theta / |z| W) \theta + ((|z| - L_c/2) \cos \theta / r_c W) z, \quad (2)$$

for $(L_c/2) - W \leq |z| \leq L_c/2$,

in each loop element 14 of width W , and

$$J = (-\cos \theta / r_c) z, \text{ for } |z| < (L_c/2) - W. \quad (3)$$

The magnetic scalar potential (ϕ_m) inside the coil obtains from matching the separate solutions from Laplace's equation to a Fourier decomposition of the currents:

$$\phi_m(r, \theta, z) = \int_0^\infty A(k) k r_c K_1(k r_c) I_1(k r) \sin \theta \cos(k z) dk \quad (4)$$

with

$$A(k) = (2 \cos k(L_c/2 - W) - 2 \cos(L_c/2)) / \pi k^2 \Delta z \quad (5)$$

where K_1 is a derivative of a modified Bessel function of the second kind with respect to the total argument. The RF magnetic field $B_1(r, z)$ is then obtained by numerical computation of the magnetic field transverse component, in a space of permeability μ_0 , so that

$$B(r, \theta, z) = -\mu_0 \nabla \phi_m. \quad (6)$$

The total effective NMR noise resistance R comprises contributions from both the coil and the sample. We consider only the contributions to noise resistance R from sample losses, as coil losses can be rendered relatively small. Again invoking reciprocity,

$$R = \sigma \int \langle \mathbf{E} \cdot \mathbf{E} \rangle dV = \frac{\sigma}{2} \int \mathbf{E} \cdot \mathbf{E} dV \quad (7)$$

where σ is the average conductivity of the sample (and is assumed to be uniform), \mathbf{E} is the electric field induced in the sample by a time-dependent magnetic field $\mathbf{B} \cos(\omega t)$ produced by a unit coil current I_1 , and the volume integral extends over the entire sample. We deduce \mathbf{E} from Faraday's law,

$$\nabla \times \mathbf{E} = -\partial \mathbf{B} / \partial t \quad (8)$$

and equation (6), as

$$\mathbf{E} = -\nabla \phi_e + (\mu_0 \omega \int_0^\infty (A(k)/k r) I_1(k r) \cos \theta \sin(k z) dk) \mathbf{r} \quad (9)$$

$$- (\mu_0 \omega \int_0^\infty A(k) I_1'(k r) \sin \theta \sin(k z) dk) \theta \quad (10)$$

with the time dependent $\sin(\omega t)$ factors suppressed, and where

$$\phi_e = \mu_0 \omega \int_0^\infty (A(k) I_1(k r_s) / k^2 r_s) I_1'(k r_s) I_1(k r) \cos \theta \sin(k z) dk, \quad (10)$$

assuming the boundary condition of no current flow normal to the sample surface at sample radius r_s , and also that the magnet fields associated with the induced currents do not themselves significantly alter the RF magnetic field B_1 . The sample noise resistance R is obtained by substitution of equa-

tions (5), (9), and (10) in equation (7), and numerical integration.

Referring now to Figure 2, the achieved NMR signal-to-noise ratio $SNR_a = B_1 / \sqrt{R}$, at the center of the coil (for $X=0$, $Y=0$ and $Z=0$) is plotted along ordinate 22 as a function of coil length L_c , which is plotted along abscissa 24 for several values of coil radius r_c , where both the coil length and coil radius are in terms of the effective radius r_s of the sample within the coil. The SNR values are seen to depend upon the ratio of the coil radius r_c and sample radius r_s ; within the desirable range from about $r_c/r_s = 1.0$ to about 1.6, the five curves 25, 26, 27, 28 and 29 respectively represent ratios of 1.1, 1.2, 1.3, 1.4 and 1.5. The effective sample radius r_s will not only depend upon the size of the sample, but also the sample shape; portions of human anatomy, such as the head, may appear, within the coil, as a RF load having an effective radius r_s different from any major dimension of that anatomical portion. It will be seen that coil radius r_c is a relatively insignificant factor affecting SNR when sample noise is dominant. It will also be seen that the normal coil length L_c of about $4r_s$, as shown at point A, has a relative SNR_a of about 0.6, which can be improved by approximately 50 percent, to a value of SNR_a of about 0.9, at point B, by shortening the coil to a length of about $L_c = 1.4r_s$. It will also be seen that a further shortening of the coil length to about $L_c = 1.0r_s$, at point C (with a coil radius r_c of about 1.1), has a relative SNR_a in excess of 1.0, and provides at least 65 percent higher SNR, relative to the SNR_a value at point A, for the normal long coil. The use of quadrature operation can add an additional 40%, so that SNR improvement of 100%, or better, is possible, relative to a single-fed, long birdcage RF coil.

Referring now to Figure 3, a relative signal-to-noise ratio sensitivity S is plotted along ordinate 32 for various values of normalized radial distance (r/r_s) from the Z axis of the cylindrical coil 10, and for values, along abscissa 34, of various normalized axial distances (z/r_s) from the coil center, $z=0$, in either direction towards the coil ends, for a particular coil having a coil radius $r_c = 1.4r_s$. It will be seen that the aforementioned 50 percent SNR increase, to a SNR_a value of 0.9 at point B (relative to a SNR_a of 0.6 at point A), is obtained at all locations along the $S=0.9$ curve 36, and that even greater relative SNR values S can be obtained closer to the center of the coil and/or at radially increased distances from the coil axis. Thus, it is seen that the penalty paid in RF magnetic field B_1 inhomogeneity is relatively modest, amounting to about 33 percent in the ($r, z=0$) plane and in transaxial planes out to about $z=0.75r_s$. Since the NMR flip angle α produced by a RF excitation field B_1 is proportional to the magnitude of the B_1 field,

and the magnetization is proportional to $\sin \alpha$, such inhomogeneity would result in only about a 13 percent loss in signal, at worst, at the center of the sample, if flip angle α were set at 90° at the sample surface, notwithstanding spin lattice relaxation effects. Therefore, this short volume coil design, with length L_c being less than $2r_s$, for r_c/r_s between about 1.0 and about 1.6, is well suited for both NMR sample excitation and response signal reception. It will also be seen that additional reduction of the coil length, to L_c less than $1.0r_s$, may provide marginally additional enhancement in SNR ψ , particularly if the coil radius r_c is also maintained at values between about $1.0r_s$ and about $1.6r_s$. We have, however, found that additional gain in SNR cannot be realized in practice, as L_c approaches zero, because the originally-assumed condition (that the sample noise dominates) cannot be obtained; as L_c approaches zero, the RF magnetic field B_1 decreases faster than the coil noise contributions. Also, because the coil radius r_c must be chosen to accommodate a range of human subjects and their non-cylindrical anatomies, it may be difficult to maintain the coil radius r_c in the range of $1.0r_s$ to $1.6r_s$.

Referring now to Figure 4, a presently preferred embodiment of a low-pass RF volume NMR coil assembly 10' is supported by a non-magnetic, non-conducting and non-dielectric tube 11', having a radius R' and a length L' which, for a coil devoid of end rings (which are not needed, as no interfering resonances are encountered at nearby frequencies), is slightly longer than the effective coil length L_c . The axis of cylindrical coil form 11' is aligned with the Z axis and the center $Z=0$ of that system is at the axial center of the coil. An antenna portion 12' is comprised of first and second spaced-apart conductive loop elements 14'a and 14'b, each having the same width W as in coil 10 of Figure 1. The effective length L_c of the coil and the radius R' are both about 5 inches. Each of conductors 14'a and 14'b is broken at each of a plurality M of locations, typically in axial alignment, by a small gap 14'c so as to form a like plurality M of substantially identical conductive segments 14's. Advantageously, the number M of segments is represented by a power q of base 2, i.e. $M=2^q$, where $q=1, 2, 3, \dots$. In the illustrated embodiment, $q=2$ and $M=4$. Each of the conductor gaps 14'c is bridged with a serially-connected capacitive element 16'. Each of another plurality N (here, equal 16) of axial conductive elements 14'e are disposed perpendicular to similarly disposed segments 14's of the first and second spaced-apart loop elements 14'a and 14'b; each axial conductive element 14'e has a width W' , here, about one-half inch. The ends of each element 14'e are separated from the adjacent segments 14's by one of gaps 14'f; each gap 14'f is

bridged by a capacitive element 40.

This particular low-pass "birdcage" form of optimized-SNR volume RF coil 10' has a feedpoint 44a at an element 14'g-1, which is separated from element 14'e-1 by a gap 14'f bridged by a capacitor 42. The unbalanced feedpoint connector 44a has the shield thereof connected to segment 14's-1 and its center conductor connected via conductor 46 to element portion 14'g-1. For quadrature excitation, a second unbalanced feedpoint 44b is located 90° from the first feedpoint 44a.

In use, a presently preferred embodiment 10', as illustrated with 5 inch coil radius $R = r_c$ and 5 inch length L_c for a sample radius r_s of about 3.5 inches, was utilized for NMR sample excitation and response signal detection. The coil was operated in the true-quadrature mode by connection of a 0° input to connector 44a and a 90° input to connector 44b, i.e. with $\theta = 90^\circ$ spacing, to provide an additional $\sqrt{2}$ improvement in SNR ψ and a two-fold reduction in the necessary excitation pulse power. The spectral SNR ψ of a 20ml. sample of 1M H_3PO_4 , located at the coil center ($z=0$ and $r=0$), was 28, as recorded from a single free-induction-decay (FID) in a bandwidth of 2KHz., with a 12Hz. line-broadening exponential filter and with the coil load adjusted, by connection of a resistor of the appropriate value across the coil inputs, to be equivalent to that load provided by a human head. The broadened full-width-half-maximum H_3PO_4 line width was 54Hz. The corresponding value of SNR ψ , obtained with a ^{31}P surface coil with a radius of 6.5 centimeters and distributed capacitance design, for a loaded head equivalent, was 18, with the phosphate sample located both on the surface coil axis and at a depth of 6.5 cm. from the coil (depth equal to coil diameter); a SNR ψ value of 56 was obtained at a depth of 3.8 centimeters. Loaded and unloaded coil quality factors (Q) were respectively 410 and 100 for the short birdcage coil, and were respectively 430 and 130 for the surface coil, at resonance; resonant frequency changes of the loaded coils were negligible. These values indicate that the relative contributions of sample noise to total detected noise were similar, being about 76% for the short birdcage coil and about 70% for the surface coil.

While several presently preferred embodiments of our novel short volume coil with optimized SNR, have been described herein, many variations and modifications will now become apparent to those skilled in the art. For example, while the analysis, supra, applies specifically to the high-pass and low-pass birdcage coils of Figures 1 and 4, respectively, because of the assumption of relatively good azimuthal field homogeneity (i.e. uniformity of field with respect to polar angle θ), the basis of this analysis is equally as well applicable to other trans-

verse coils, such as solenoidal, saddle and sinusoidal designs, with and without distributed capacitance (i.e., most coils producing an RF field in a direction substantially perpendicular to the main static magnetic field in which the RF coil is immersed), as known to the art; these designs can all provide SNR benefit when L_c and r_c are chosen according to the invention, i.e. $0.3r_s \leq L_c \leq 1.5r_s$ and $1.0r_s \leq r_c \leq 1.6r_s$.

Accordingly, preferred embodiments of the present invention provide a volume RF coil, for use in NMR and the like systems, having an improved signal-to-noise ratio.

Claims

1. A radio-frequency (RF) volume coil, for at least one of excitation and reception of NMR response signals from a sample having an effective radius r_s comprising:
a tube of an insulative material and having exterior surface; and
a conductive, generally cylindrical, antenna fabricated upon said exterior surface with a radius r_c which is between about 1.0 r_s and about 1.6 r_s and an effective length L_c of less than 2 r_s , and having a signal-to-noise ratio (SNR), when said sample is enclosed within said antenna, greater than the SNR of a similar antenna having the same radius r_c and an effective length of at least 4 r_s .

2. The RF volume coil of claim 1, wherein the antenna has first and second feedpoints positioned for quadrature response signal reception.

3. The RF volume coil of Claim 1, wherein the antenna is of a birdcage form, including: first and second spaced-apart conductive loop elements, each located in a plane substantially perpendicular to the axis of the tube and broken by a plurality of substantially equally spaced gaps into a like plurality of conductive segments and with each of a second plurality of parallel conductive axial elements disposed and coupled between a like positioned segment in each of the first and second loop elements; a different one of a plurality of capacitive elements serially connected across a different associated one of the gaps in each of the first and second loop elements; and means for providing a first feedpoint at a selected location along one of the loop elements.

4. The RF volume coil of Claim 3, wherein each of the loop element conductors has a width W substantially equal to the width W' of each axial element.

5. The RF volume coil of Claim 4, wherein width W is about one order of magnitude less than the coil length L_c .

6. The RF volume coil of Claim 3, 4 or 5, wherein the antenna is of a high-pass birdcage form.

7. The RF volume coil of Claim 3, 4 or 5, wherein the antenna is of a low-pass birdcage form.

8. The RF volume coil of Claim 3, 4, 5, 6 or 7, further comprising means for providing another feedpoint at another selected location along the same loop element.

9. The RF volume coil of Claim 8, wherein the another feedpoint has an electrical separation of about 90 degrees from the first feedpoint.

10. The RF volume coil of any preceding claim, wherein the coil radius r_c is on the order of 5 inches.

11. The RF volume coil of Claim 10, wherein the coil effective length L_c is on the order of 5 inches.

12. The RF volume coil of any one of Claims 1-9, wherein the effective length L_c is between about $0.3r_s$ and about $1.5r_s$.

13. The RF volume coil of any one of Claims 1-9 and 12, wherein the antenna radius r_c is between about $1.1r_s$ and about $1.5r_s$.

14. The RF volume of any one of claims 1-9 and 12 and 13, wherein the effective length L_c is between about $1.0r_s$ and about $1.4r_s$.

5

10

15

20

25

30

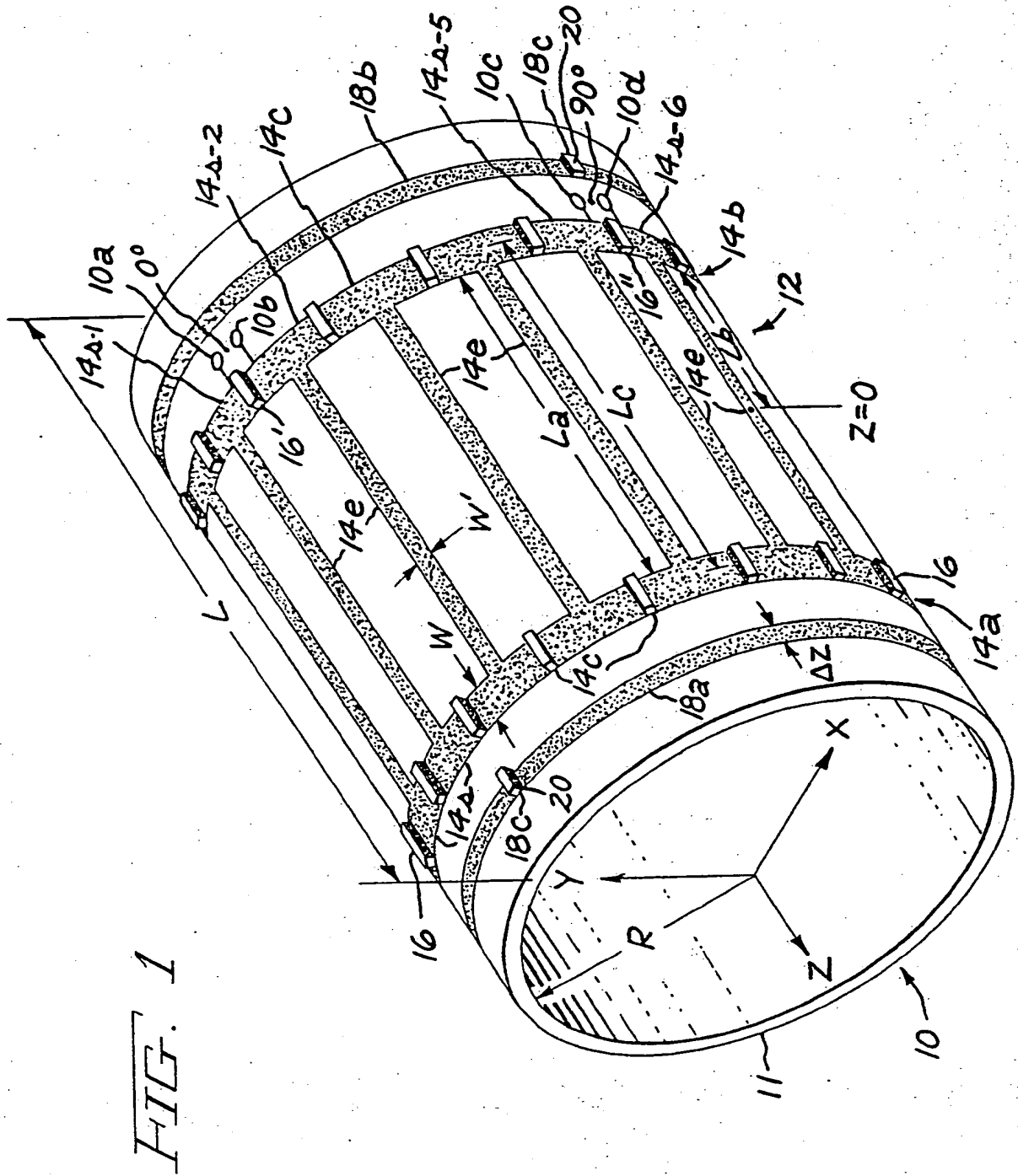
35

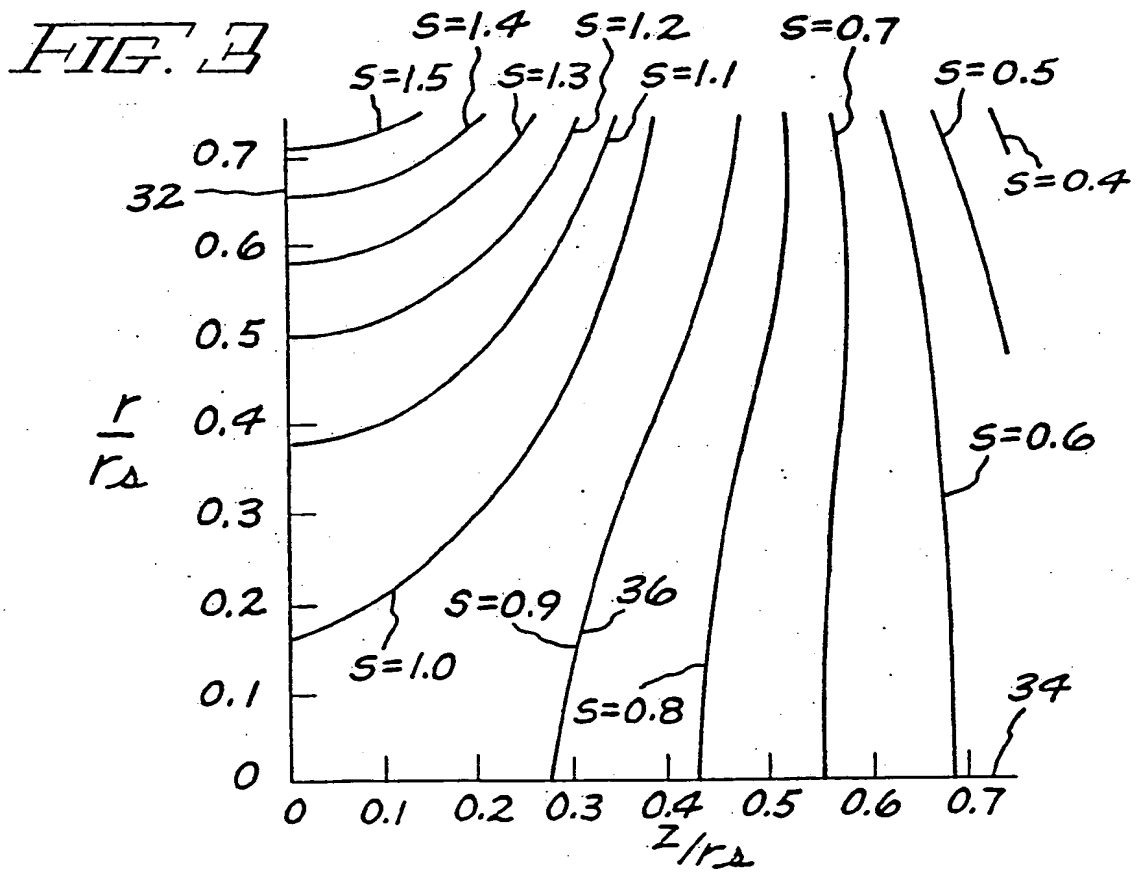
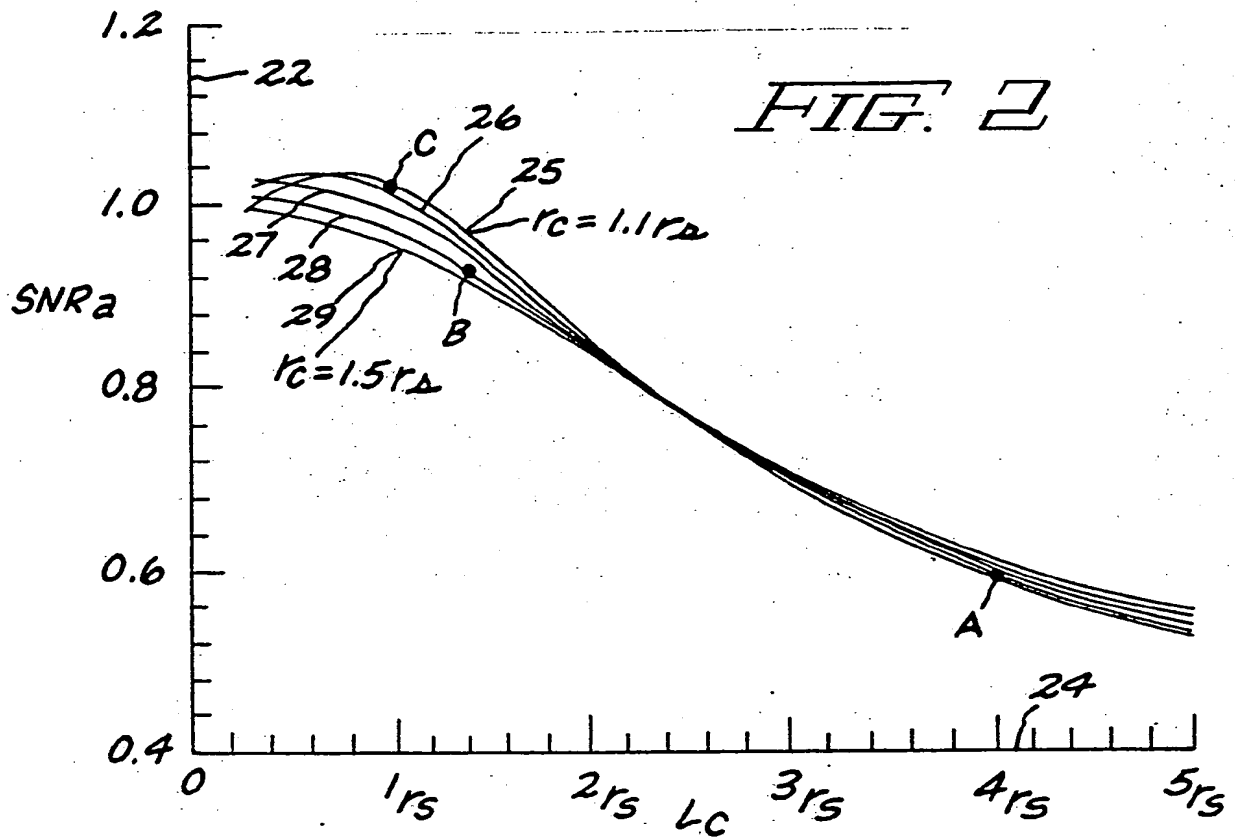
40

45

50

55







(19)



Europäisches Patentamt
European Patent Office
Office européen des brevets



(11) Publication number:

0 346 049 A3

(12)

EUROPEAN PATENT APPLICATION

(21) Application number: 89305663.0

(51) Int. Cl.⁵ **G01N 24/04**

(22) Date of filing: 05.06.89

(30) Priority: 06.06.88 US 202624

(43) Date of publication of application:
13.12.89 Bulletin 89/50(84) Designated Contracting States:
DE FR GB NL(86) Date of deferred publication of the search report:
16.01.91 Bulletin 91/03(71) Applicant: **GENERAL ELECTRIC COMPANY**
1 River Road
Schenectady, NY 12345(US)

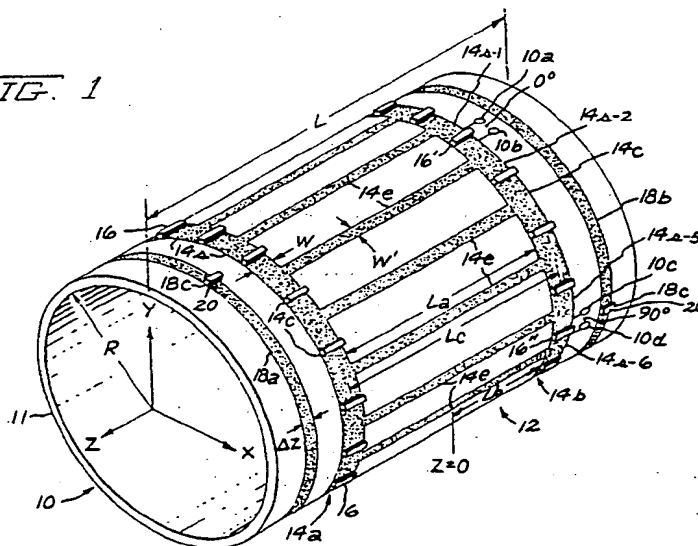
(72) Inventor: **Roemer, Peter Bernard**
955 Saint David's Lane
Schenectady New York 12309(US)
Inventor: **Bottomley, Paul Arthur**
64 Pico Road
Clifton Park New York 12065(US)
Inventor: **Edelstein, William Alan**
850 Oregon Avenue
Schenectady New York 12309(US)

(74) Representative: **Pratt, Richard Wilson et al**
London Patent Operation G.E. TECHNICAL
SERVICES CO. INC. Burdett House 15/16
Buckingham Street
London WC2N 6DU(GB)

(54) RF coil for NMR.

(57) A RF volume coil with optimized signal-to-noise ratio, for NMR use, has a reduced length L_c , which is between about $0.3r_s$ and about $1.5r_s$, where r_s is the radius of a sample-to-be-investigated, contained within the cylindrical volume coil, with the volume

coil radius r_c being between about $1.0r_s$ and about $1.6r_s$. The "short" volume coil has an improved SNR for a voxel located substantially on the central plane of the coil, relative to the SNR of a "normal"-length volume coil with $L_c \geq 4r_s$.

FIG. 1**EP 0 346 049 A3**



European
Patent Office

EUROPEAN SEARCH REPORT

Application Number

EP 89 30 5663

DOCUMENTS CONSIDERED TO BE RELEVANT

Category	Citation of document with indication, where appropriate, of relevant passages	Relevant to claim	CLASSIFICATION OF THE APPLICATION (Int. Cl.5)
A	MAGNETIC RESONANCE IN MEDICINE, vol. 3, no. 4, August 1986, pages 604-618, New York, US; W.A. EDELSTEIN et al.: "The intrinsic signal-to-noise ratio in NMR imaging" * Page 604, line 1 - page 607, line 5 *	1,10-14	G 01 N 24/04
D,A	US-A-4 692 705 (C.E. HAYES) * Column 2, lines 56-68; column 4, line 36 - column 5, line 41; column 9; line 45 - column 10, line 20; figure 2b *	1-10	
D,A	US-A-4 680 548 (W.A. EDELSTEIN et al.) * Column 4, lines 4-34; column 8, line 1 - column 9, line 25; figures 2a,3a *	1-3,6-10	
P,A	REVIEW OF SCIENTIFIC INSTRUMENTS, vol. 59, no. 6, June 1988, pages 926-929, New York, US; J.C. WATKINS et al.: "High-pass bird-cage coil for nuclear-magnetic resonance" * Whole article *	1-3,6,7	
The present search report has been drawn up for all claims			TECHNICAL FIELDS SEARCHED (Int. Cl.5)
			G 01 N G 01 R
Place of search		Date of completion of search	Examiner
The Hague		06 November 90	VOLMER J.W.
CATEGORY OF CITED DOCUMENTS			
X : particularly relevant if taken alone		E : earlier patent document, but published on, or after the filing date	
Y : particularly relevant if combined with another document of the same category		D : document cited in the application	
A : technological background		L : document cited for other reasons	
O : non-written disclosure			
P : intermediate document		& : member of the same patent family, corresponding document	
T : theory or principle underlying the invention			

**This Page is Inserted by IFW Indexing and Scanning
Operations and is not part of the Official Record**

BEST AVAILABLE IMAGES

Defective images within this document are accurate representations of the original documents submitted by the applicant.

Defects in the images include but are not limited to the items checked:

- ☐ **BLACK BORDERS**
- ☐ **IMAGE CUT OFF AT TOP, BOTTOM OR SIDES**
- ☐ **FADED TEXT OR DRAWING**
- ☐ **BLURRED OR ILLEGIBLE TEXT OR DRAWING**
- ☐ **SKEWED/SLANTED IMAGES**
- ☐ **COLOR OR BLACK AND WHITE PHOTOGRAPHS**
- ☐ **GRAY SCALE DOCUMENTS**
- ☐ **LINES OR MARKS ON ORIGINAL DOCUMENT**
- ☐ **REFERENCE(S) OR EXHIBIT(S) SUBMITTED ARE POOR QUALITY**
- ☐ **OTHER:** _____

IMAGES ARE BEST AVAILABLE COPY.

As rescanning these documents will not correct the image problems checked, please do not report these problems to the IFW Image Problem Mailbox.